Desalination and Water Treatment
www.deswater.com

doi:10.5004/dwt.2019.23301

139 (2019) 228–245
January

Enhanced uptake of gold ions from wastewater due to covalent functionalization of organotriphosphonic acid on japonica shells

Lijun Wei, Ping Yin*, Zhenglong Yang*, Yanbin Xu, Wei Jiang, Juan Jin, Honglan Cai, Zhenliang Guo

School of Chemistry and Materials Science, Ludong University, Yantai 264025, China, Tel. 86-18254559867, Fax 86-535-6697667, email: lduweilijun@163.com (L. Wei), Tel + 86-535-6696162, Fax + 86-535-6697667, e-mail: yinping426@163.com (P. Yin), Tel. 86-13695352875, Fax 86-535-6697667, email: yzl@iccas.ac.cn (Z. Yang), Tel. 86-15953542833, Fax 86-535-6697667, email: xuyb_lzu@hotmail.com (Y. Xu), Tel. 86-15153523961, Fax 86-535-6697667, email: jweicn@163.com (W. Jiang), Tel. 86-13002726239, Fax 86-535-6697667, email: jinjuan8341@163.com (J. Jin), Tel. 86-15866451889, Fax 86-535-6697667, email: honglancai@163.com (H. Cai), Tel. 86-13884933549, Fax 86-535-6697667, email: guozhenliang51@sohu.com (Z. Guo)

Received 11 April 2018; Accepted 18 October 2018

ABSTRACT

In the present work, the facile covalent functionalization of organotriphosphonic acid on japonica shells (OTPA-JS) has been developed and they were used for enhanced uptake of gold ions from wastewater. The theoretical calculations of the cellulose with organotriphosphonic acid group have been carried out at the B3LYP/6-31+G(d) level to design the bioabsorbent material OTPA-JS. The studies on the adsorption properties of japonica shells JS and OTPA-JS for Au(III), Hg(II), Cu(II), Pb(II), Ni(II), Co(II), Zn(II), Cr(III) and Cd(II) have revealed that OTPA-JS displayed excellent enhanced adsorption for gold ions compared to JS. Furthermore, the adsorption selectivity results showed that OTPA-JS had strong affinity for gold ions in the aqueous solutions and even exhibited 100% selectivity for Au(III) ions in the presence of Co(II), Zn(II), Cr(III) and Cd(II). The relevant adsorption behaviors of OTPA-JS and JS for gold ions, such as the effect of pH value, the adsorption kinetics, and thermodynamics as well, have also been investigated. The results indicated the maximum adsorption capacities of OTPA-JS at 35°C could reach 523.56 mg/g, the activation energy value for Au(III) onto OTPA-JS was –38.82 kJ/mol, and the adsorption thermodynamic parameters ΔG, ΔH and ΔS were –103.03 kJ·mol^{-1}, 96.87 kJ·mol^{-1}, and 334.82 J· K^{-1}·mol^{-1}, respectively. Moreover, the adsorption mechanism for gold ions adsorption was also investigated, which were based on the results of FTIR, XPS, SEM, and XPS of the sample after gold ions adsorption (OTPA-JS-Au). Moreover, this modified adsorbent was utilized to uptake gold ions in the gold-plating wastewater samples. Therefore, the prepared adsorbent OTPA-JS is expected to be a new biomass material for the uptake and recovery of gold from contaminated water.

Keywords: Gold ions uptake; Japonica shells; Covalent functionalization; Organotriphosphonic acid; Adsorption mechanism

1. Introduction

Gold, as one of the precious metals and a global currency, has been utilized in a lot of industrial and medical fields because of its special physical and chemical properties. Correspondingly, the recover gold form industrial scraps and wastewater such as mining, electronics and electroplating has recently been an international concern due to its value and scarcity, and the environmental pollution as well. Therefore, the effluents from these scrap industry containing gold ions have drawn considerable attention. This has provided a compelling reason for developing effective treatment methods for recovering and reuse of gold ions [1]. Adsorption is a kind of highly efficient, economical and

*Corresponding author.

easily regenerated ways for the removal of metal ions from wastewaters compared to the conventional treatment methods [2–7]. Therefore, adsorption method is often considered in the processes of gold uptake from aqueous solutions, especially when the adsorbent is inexpensive and readily available [8,9]. Recently, biosorption using agricultural wastes has been regarded as a promising technology for efficient and fast process of gold ions uptake at lower cost compared with other methods [10,11].

Japonica is an important rice subspecies in Asia, it is mainly distributed in Northeast China and accounts for 44.6% of the total cultivated area of japonica rice in China [12]. Generally, the agricultural waste japonica shells are generated on site as a kind of byproduct in the milling factories during the production of rice. The world production of japonica shells is estimated to be several million tons every year, therefore, the disposal of these vast amounts of them has been one major problem. Reusing this agricultural waste product is one goal of environmental sustainability. It seems a reasonable assumption that the agricultural waste presents great potential use in large scale, such as adsorbent and composite industries [13]. As a kind of agricultural waste, japonica shells are rich in cellulose with hydroxyl functional groups, and they could be selected to be applied as absorbent material in the present work. In order to develop the innovative low-cost adsorbents with good affinity towards targeted metal ions, the preparation strategy of effective surface modification technology with function groups should betaken [14].

Japonica shells are available in large quantity, and organophosphonic acids have good coordination property. Concerning the above-mentioned ideas, the objective of this work was to effectively enhance the adsorption capability of biomass-based adsorbents for gold ions by covalent chemical modification of japonica shells with organotriphosphonic acid. The motivation of the present work is to explore the possibility of utilizing OTPA-JS for the bioadsorption of gold ions from wastewater. Covalent functionalization with ligand such as organotriphosphonic acid on the surface of japonica shells is sure to obtain specific adsorption and larger capacity. The effect of such experimental factors as adsorbent dose, pH, contact time, initial concentration and temperature were investigated in detail. The adsorption kinetics of gold ions onto JS and OTPA-JS was analyzed by fitting various kinetic models. Experimental equilibrium data were fitted to the Langmuir and Freundlich equations, and the error analysis was conducted to test the adequacy and the accuracy of the model equations. Thermodynamics of the adsorption process has been studied, and the change in Gibbs free energy, the enthalpy and the entropy of adsorption have also been determined, which are important parameters for the design of any industrial adsorption system. In addition, the adsorption mechanism of OTPA-JS for gold ions has been investigated, and it was also utilized to uptake gold ions in the gold-plating wastewater samples.

2. Experimental details

2.1. Materials and instruments

The spent japonica rice shells obtained from Northeast China were thoroughly washed and dried at 40°C, and they were ground and passed through a 120 mesh sieve to obtain the uniform particle size (JS).10.0 g of JS was agitated at 60°C for 24 h in 40 mL of organotriphosphonic acid (aminotrimethylenephosphonic acid) solution. The resulting biomasses were filtered and dried, then, the treated sample was thermochemically reacted at 120°C for 4 h. The products obtained were mixed in deionized water for 30 min, then filtered, and washed with deionized water three times. Finally, organotriphosphonic acid modified japonica shells (OTPA-JS) were dried in the vacuum oven at 45°C for 48 h. All the analytical chemicals were purchased from Sinopharm Chemical Reagent (Shanghai) Co. Ltd., and used as received without further purification, and all solutions were prepared with deionized water. Stock solutions of containing various metal ions at a certain concentration were prepared by dissolving their relative metal salts in deionized water.

Infrared spectra (FT-IR) of samples were reported in the range of 4000–400 cm^{-1} with a resolution of 4 cm^{-1}, by accumulating 32 scans using a Nicolet MAGNA-IR 550 (series II) spectrophotometer. The morphology of the products was examined on JEOL JSF5600LV scanning electron microscope. Thermogravimetric analysis (TG) was recorded on a Netzsch STA 409, Test conditions: type of crucible, DTA/TG crucible Al_2O_3; nitrogen atmosphere, flow rate 30 mL/min; heating rate: 10 K/min. Powder X-ray diffraction (XRD) data were obtained using a Rigaku Max-2500VPC diffractometer (Rigaku Co., Japan) with Cu-Kα_1 radiation (λ = 1.54056 Å). The XPS (X-ray photoelectron spectroscopy) measurement was made on a Perkin-Elmer PHI 550-ESCA/SAM photoelectron spectrometer operated at 10 kV and 30 mA. High resolution XPS spectra were generated with the analyzer pass energy setting at 10 and 50 eV, respectively. Atomic absorption analysis of transition metal ions was performed with a flame atomic absorption GBC-932A spectrophotometer (GBC Co., Australia).

2.2. Computational details

Theoretical calculations of the cellulose with aminotrimethylenephosphonic acid group have been performed with the Gaussian 03 program [15] using the B3LYP/6-31+G(d) basis set to obtain the optimized molecular structure and vibrational wavenumbers. The frequencies for the required structure were evaluated at the B3LYP/6-31+G(d) level to ascertain the nature of stationary points, and the harmonic vibrational wavenumbers were calculated using the analytical second derivatives to confirm the convergence to a minimum of the potential surface. Moreover, Mulliken atomic charges of the cellulose with organotriphosphonic acid group were also obtained at the B3LYP/6-31+G(d) level.

2.3. Biosorption experiments for heavy metals

Static adsorption experiment was employed to determine the adsorption capacities of JS and OTPA-JS for different kinds of heavy metal ions. The static adsorption experiments were carried out with shaking 20.0 mg of adsorbents with 20 mL of metal ion solution (2.0 mmol/L). The mixture was equilibrated for 24 h on a thermostat-cum-shaking assembly at 25°C.

The adsorption amount was calculated according to Eq. (1):

$$q = \frac{(C_o - C_e)V}{W} \quad (1)$$

where q is the adsorption amount (mmol/g); C_o and C_e are the initial and equilibrium concentrations of metal ions (mmol/mL) in solution, respectively; V is the volume of the solution (mL); W is the weight of JS/ OTPA-JS used (g).

2.4. Competitive adsorption

In order to investigate the adsorption selectivity of the adsorbent OTPA-JS for Au(III), 20.0 mg of the adsorbents were added into 20 mL solutions (binary system which containing equal initial concentrations (2.0 mmol/L) of Au(III) ion and other coexisting metal ions) and the mixture was shaken for 12 h. The solutions were separated from the adsorbents after adsorption behavior and the concentration of metal ions was detected by atomic absorption spectrometer.

2.5. Effect of pH on adsorption

The effect of pH on the adsorption of Au(III) was studied by adding 20.0 mg of JS/OTPA-JS adsorbent to 2.43 mol/L Au(III) at different pH values (1.5–6.0) in 100 mL Erlenmeyer flask. The mixture was equilibrated for 24 h on a thermostat-cum-shaking assembly at 25°C. The solutions were separated from the adsorbents after adsorption behavior and the concentration of gold ions was detected by atomic absorption spectrometer.

2.6. Effect of adsorbent dosage on adsorption

The effect of adsorbent on the adsorption of Au(III) was studied by adding some JS/OTPA-JS adsorbent (10.0 mg–60.0 mg) to 2.43 mol/L Au(III) at pH = 2.5 in 100 mL Erlenmeyer flask. The mixture was equilibrated for 12 h on a thermostat-cum-shaking assembly at 25°C. The solutions were separated from the adsorbents after adsorption behavior and the concentration of gold ions was detected by atomic absorption spectrometer.

2.7. Adsorption isotherms

The isotherm adsorption property of the adsorbents was also investigated by batch tests. The adsorption isotherms were studied using 20.0 mg of JS/OTPA-JS adsorbent with the various gold ion concentrations (1.21–6.07 mmol/L) at pH 2.5 and at 15–35°C for 24 h.

2.8. Adsorption kinetics

The adsorption kinetics on the uptake of Au(III) ion by the adsorbent was studied by placing 20.0 mg of OTPA-JS adsorbent with 10 mL of metal ion solution in a series of flasks at pH = 2.5 and at 5–35°C with the concentration of the metal ion being 2.43 mmol/L. At a certain time interval, the adsorbents were filtrated after adsorption behavior and the concentrations of gold ions in solutions were determined.

2.9. Adsorption of gold/copper ions from industrial wastewater

The feed solutions of the sample 1 and the sample 2 were industrial wastewater collected from the manufacture lines of gold-plating. The adsorption experiments were conducted by adding 20.0 mg of OTPA-JS adsorbents in 20 mL of metal ions solutions at ambient temperature. At a certain time interval, the adsorbent was filtrated and the concentrations of Au(III)/Cu(II) ion in solutions were determined via atomic absorption spectrometer.

3. Results and discussion

3.1. Theoretic calculations of cellulose with aminotrimethylenephosphonic acid group

The organophosphonic acids are good candidates for coordinating with metal ions, in which the organic moieties play a controllable spacer role and the phosphonic groups could coordinate with metal ions to exhibit interesting architectures and possible functionalities [16]. Aminotrimethylenephosphonic acid possessed three phosphonic acid groups and a central nitrogen atom. In the present work, the introduction of the organotriphosphonic acid groups onto spent japonica shells can make the agricultural waste form stable chelating compounds with many heavy metal ions [17]. The phosphonic acid groups can provide several oxygen atoms to coordinate metal ions. The aim of chemical modification with the designed organotriphosphonic acid, which has oxygen donor atoms in phosphonic acid functional groups, is to make the material have excellent coordination properties with metal ions and to obtain the adsorbent with a high loading capacity for metal ions. Moreover, the formation of the coordination bonds, and the interaction of organophoaphonic acid and heavy metal ions could reduce the potential risk of releasing the adsorbed heavy metal ions back into purified water.

OTPA-JS has been developed as described in the experimental details section, its preparation reaction is shown in Fig. 1. In order to design the title agricultural waste-based adsorbent material, we theoretically calculated the cellulose with aminotrimethylenephosphonic acid group at the B3LYP/6-31+G(d) level in advance, and the optimized structure of the cellulose with organotriphosphonic acid group is displayed in Fig. 2 (1), the corresponding selected bond lengths and bond angles were presented in Table S1 (available online in the supplemental materials). The P24-O25, P38-O41 and P39-O40 bond lengths are 1.5096 Å, 1.4925 Å and 1.4920 Å, respectively, which agrees with well with those values of phosphonic acid in Ref [18] and is slightly longer than the experimental value (1.47 Å). In addition, the P24-O15, P24-O26, P38-O46, P38-O48, P39-O42 and P39-O44 bond lengths are in the range (1.6030 to 1.6343) Å, comparable to those in phosphonic acid (1.59–1.63) Å [18]. Moreover, the bond angles A(28, 24, 15/25/26), A(32, 38, 41/46/48) and A(35, 39, 40/42/44) were produced with reasonable accuracy as well. Table S2 (available online in the supplemental materials) presented the Mulliken atomic charges of the modified triphosphonic acid group, and shows that the oxygen

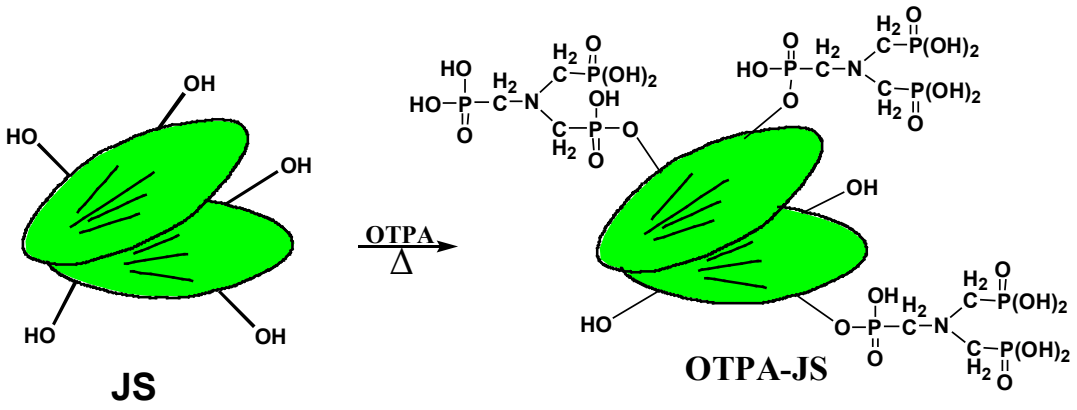

Fig. 1. The preparation reaction of the agricultural waste-based adsorbent OTPA-JS.

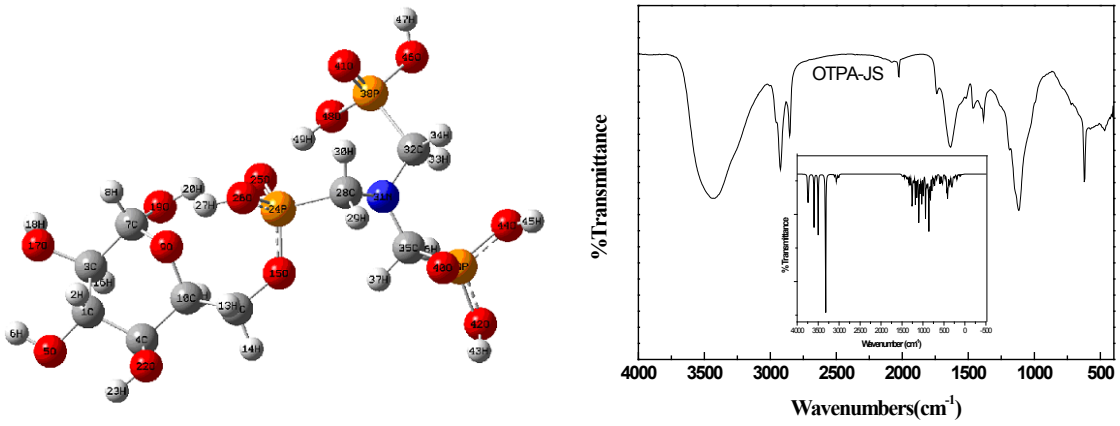

(1) (2)

Fig. 2. (1) Optimized geometry of the cellulose with organotriphosphonic acid group; (2) Experimental FT-IR spectrum of OTPA-JS and calculated IR spectrum (inset) of the cellulose with aminotrimethylenephosphonic acid at the B3LYP/6-31+G(d) level.

atoms in phosphonic acid groups have more negative charges, and the Mulliken electronic populations of O15, O25, O26, O40, O41, O42, O44, O46 and O48 were –0.602, –0.966, –0.864, –0.714, –0.714, –-0.805, –0.818, –0.841 and –0.790, respectively, which made these oxygen atoms coordinate with metal ions more easily. Therefore, the designed organic groups may provide a good adsorbent for the use in adsorbing metal ions from aqueous solutions. In addition, the observed and calculated IR spectrum is shown in Fig. 2 (2). In the calculated spectrum, the peaks at 3500–3300 cm^{-1} were assigned to –OH stretching vibration, their peaks at 3100–3000 cm^{-1} were attributed to symmetric and asymmetric stretching vibration of $–CH_2$, and the peaks at 1000–800 cm^{-1} should be assigned to the skeletal vibration concerning the $–PO_3H_2$ groups. It could be seen that the calculated harmonic frequencies were a little larger than those experimental values. It is known that the calculations consistently overestimate the vibration frequencies, scaling the calculated harmonic frequencies could improve agreement with experiment [19]. After correcting these discrepancies by scaling the calculated wavenumbers with a 0.977 factor [20], the theoretical frequencies were in good agreement with the observed results.

3.2. Characterization of OTPA-JS

The aminotrimethylenephosphonic acid functional groups and structures on the surface of the adsorbent strongly affect its heavy metal adsorption capacity. Fig. 3(1) represents all the diffraction peaks of JS and OTPA-JS, and their XRD patterns indicated the amorphous nature of the material lacking any crystallinity. The result also showed that there was no an essential change occurred in topological structure of JS before and after the modification reaction with aminotrimethylenephosphonic acid, which implied that JS was stable enough to experience the chemical modification reactions. No new diffraction peak appeared after the facile preparation reaction meant that the modified function groups on the surface of JS existed in a form of non-crystalline state. XRD data showed that the organotriphosphonic acid treatment does not alter the structure of japonica shells. Fig. 3(2) shows SEM photographs of JS (inset) and OTPA-JS at 2000 times magnification. It is obvious that the surface of JS became rougher after the modification. More cavities on the surface of OTPA-JS might increase the contact areas and facilitate diffusion during adsorption process, which could improve its adsorption ability for metal ions from

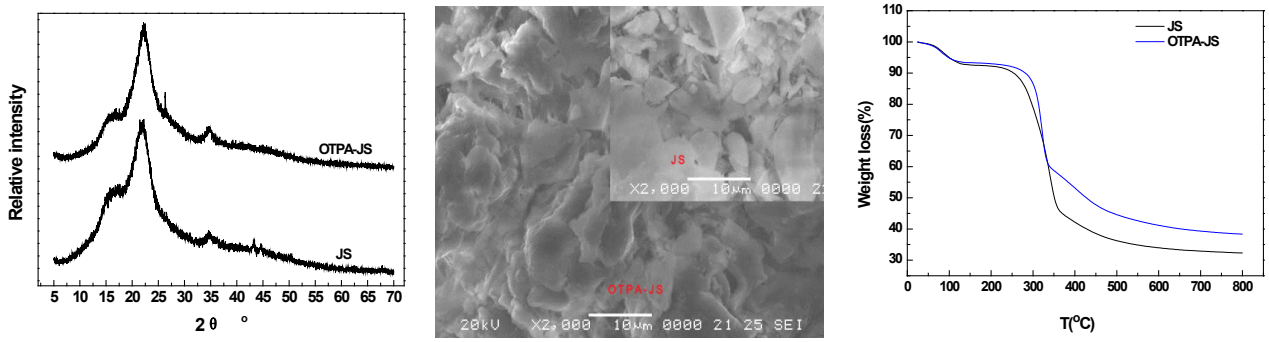

(1) (2) (3)

Fig. 3. (1) XRD patterns of JS and OTPA-JS; (2) SEM image of JS (inset) and OTPA-JS; (3) TG curves of JS and OTPA-JS.

aqueous media [20]. As expected, the organotriphosphonic acid functionalization does not lead to any observable surface changed as the functionalization is only a surface treatment. The particle appearances of these samples were similar, demonstrating that the particles of OTPA-JS had good mechanical stability and they had not been destroyed during the covalent functionalization reaction. The TG curve could reflect the thermal stability of the material, and the thermal stability of JS andOTPA-JS has been determined by thermal analysis, and the result is shown in Fig. 3(3). The thermal analysis represented several steps of decomposition in the temperature range of 25–800°C. The weight loss of 7.78 and 7.02% in the temperature range of 25–200°C corresponded to the release of physically adsorbed water in JS and OTPA-JS, respectively. Further weight loss above 200°C is due to the decomposition of the organic function groups. It is noted that there is almost no weight loss for OTPA-JS at 25–50°C, and the adsorbents usually are utilized below 50°C. As a result, these data indicated that the resulting product OTPA-JS had good thermal stability and it should be applied at the temperature below 50°C, and it could be expected that OTPA-JS could present an adequate chemical and physical characteristics to adsorb metal ions due to the introduction of organotriphosphonic acid groups.

3.3. Saturated adsorption for heavy metals

Saturated adsorption capacities for heavy metal ions were essential parameters for evaluating the adsorption ability of the adsorbents. Fig. 4 shows the static adsorption capacities of JS and OTPA-JS for Au(III), Hg(II), Cu(II), Pb(II), Ni(II), Co(II), Zn(II), Cr(III) and Cd(II) metal ions. Japonica shells without chemical modification have the adsorption ability for metal ions to some extent, and the static adsorption capacities of JS for Au(III), Hg(II) and Cu(II) were 0.34 mmol/g, 0.52 mmol/g, and 0.43 mmol/g, respectively, and those for Pb(II), Ni(II), Co(II), Zn(II), Cr(III) and Cd(II) metal ions were 0.33 mmol/g, 0.29 mmol/g, 0.34 mmol/g, 0.22 mmol/g, 0.17 mmol/g and 0.38 mmol/g, respectively. As is seen from Fig. 4, organotriphosphonic acid functional groups presenting in the biopolymer structure of japonica shells have obvious influence on the adsorption capacities for heavy metal ions in the aqueous solutions. The surface modification could further provide binding sites and

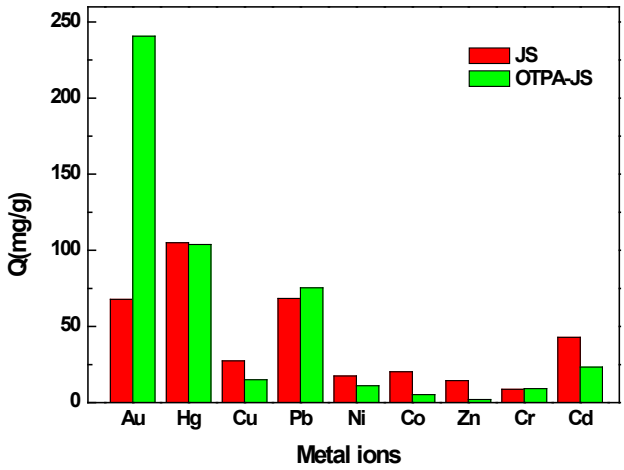

Fig. 4. The saturation adsorption capacities of JS and OTPA-JS for heavy metal ions (20 mL, 2.0 mmol/L of initial solution, 25°C).

greatly improve the adsorption properties for some particular metal ions, especially for Au(III) ions from aqueous solutions. The adsorption capacities of JS and OTPA-JS for Au(III) ions were 0.34 mmol/g and 1.22 mmol/g, respectively. The gold ions adsorption capacities of japonica shells was greatly enhanced after the functionalization of organotriphosphonic acid, OTPA-JS has the highest adsorption capacities for Au(III), and the phosphonic acid functional groups on the surface of japonica shells might possess high affinity for gold ions.

3.4. Adsorption selectivity

The most important properties of an adsorbent material that influence its application are adsorption amount in addition to sorption selectivity which is basically an attribute of the functional groups of the adsorbent. Therefore, the adsorption selectivity is an indispensable factor for evaluating the capacities of an adsorbent, by which the adsorbent can be used to adsorb a specific transition metal ions or to separate specific transition metal ions from a mixed metal

ions solution. In this study, the adsorption selectivity experiments by OTPA-JS were carried out from Au(III)-Hg(II), Au(III)-Cu(II), Au(III)-Cd(II), Au(III)-Pb(II), Au(III)- Ni (II), Au(III)- Co(II), Au(III)- Zn(II), Au(III)-Cr(III), and Au(III)–Cd(II) binary systems. The obtained results for gold(III) adsorption at 25°C are presented in Table 1. The selective coefficient was the ratio of adsorption capacities of metal ions in binary mixture:

The selective coefficient $= \frac{q'}{q''}$, where q' is adsorption capacities of Au(III)ion in binary mixture and q'' is adsorption capacities of the other metal ion in binary mixture. The results displayed that OTPA-JS had excellent adsorption for Au(III) in binary ions systems, especially in the systems of Au(III)–Co(II), Au(III)–Zn(II), Au(III)–Cr(III), and Au(III)–Cd(II). The investigation on the adsorption selectivity showed that OTPA-JS displayed strong affinity for gold in the aqueous solutions and exhibited 100% selectivity for gold ions in the presence of Co(II), Zn(II), Cr(III) and Cd(II). As a result, this novel organotriphosphonic acid-modified japonica shell adsorbent has good adsorption properties and high capacity for Au(III), which can be applied for uptaking this precious metal element from aqueous solutions. The above-mentioned research results show that the low-cost agricultural waste-based OTPA-JS is very favorable for the removal of precious metal ions, and the high adsorption capacity make it a good promising candidate material for Au(III) uptake. These findings suggest that OTPA-JS can probably be used in the extraction, separation and recovery of gold ions from a multi-ionic aqueous system. In the following part, the adsorption process of the japonica shells -based biomass adsorbents for gold ions was investigated particularly.

Table 1
The adsorption selectivity of OTPA-JS for Au(III) (Au(III) concentration: 2.0 mmol/L; concentration of coexisting metal ions: 2.0 mmol/L; T = 25°C)

System	Metal ions	Adsorbents capacity (mmol/g)	Selective coefficient
Au(III)–Hg(II)	Au(III)	1.07	$\alpha_{Au(III)/Hg(II)} = 51$
	Hg(II)	0.02	
Au(III)–Cu(II)	Au(III)	1.09	$\alpha_{Au(III)/Cu(II)} = 557$
	Cu(II)	0.002	
Au(III)–Pb(II)	Au(III)	1.10	$\alpha_{Au(III)/Pb(II)} = 70$
	Pb(II)	0.02	
Au(III)–Ni(II)	Au(III)	1.07	$\alpha_{Au(III)/Ni(II)} = 425$
	Ni(II)	0.003	
Au(III)–Co(II)	Au(III)	0.97	$\alpha_{Au(III)/Co(II)} = \infty$
	Co(II)	0.00	
Au(III)–Zn(II)	Au(III)	1.15	$\alpha_{Au(III)/Zn(II)} = \infty$
	Zn(II)	0.00	
Au(III)–Cr(III)	Au(III)	1.08	$\alpha_{Au(III)/Cr(III)} = \infty$
	Cr(II)	0.00	
Au(III)–Cd(II)	Au(III)	1.06	$\alpha_{Au(III)/Cd(II)} = \infty$
	Cd(II)	0.00	

3.5. Effect of pH on gold adsorption

The pH value of the metal ions solution is one of the most important factors influencing the adsorption behavior of heavy metal ions on adsorbents. It not only impacts the surface structure of adsorbents and the formation status of heavy metal ions, but it may also influence the interaction between adsorbents and heavy metal ions. Moreover, it is well known that the chemical morphology of chlorogold complexes is an important factor influencing the adsorption behavior of gold in aqueous solutions. The molar fractions of these gold species were based on various conditions, such as the chloride ion and hydrogen ion concentrations as well as the temperature. The equilibrium constants (K) of gold chloride in solutions are shown in Eqs. (2)–(5)[21]:

$$Au(OH)_4^- + H^+ + Cl^- \Leftrightarrow AuCl(OH)_3^- + H_2O \quad K = 10^{8.51} \tag{2}$$

$$AuCl(OH)_3^- + H^+ + Cl^- \Leftrightarrow AuCl_2(OH)_2^- + H_2O \quad K = 10^{8.06} \tag{3}$$

$$AuCl_2(OH)_2^- + H^+ + Cl^- \Leftrightarrow AuCl_3(OH)^- + H_2O \quad K = 10^{7.00} \tag{4}$$

$$AuCl_2(OH)_2^- + H^+ + Cl^- \Leftrightarrow AuCl_3(OH)^- + H_2O \quad K = 10^{6.07} \tag{5}$$

It is evident that the predominant complex of gold is $AuCl_4^-$ at pH < 3. Increasing the pH value of the solution would cause the hydrolysis of $AuCl_4^-$ to proceed, and thus hydrolyzed chlorogold complexes such as $AuCl_3(OH)^-$ would appear in the aqueous chloride solution. In order to evaluate the effect of the initial pH on the adsorption behavior of gold ions, the adsorption experiments were conducted in the pH range of 1.5–6.0, and the effect of pH on the adsorption for Au(III) onto JS and OTPA-JS is illustrated in Fig. 5(1). The results showed that the solution pH has a significant effect on the adsorption capacity. In the case of the adsorbent OTPA-JS, lower adsorption capacity was observed when the adsorption was carried out at lower pH (<2.5). This is because the competition adsorption between Cl^- and $AuCl_4^-$ influenced the Au(III) adsorption on the positively charged sites of OTPA-JS with high concentration of Cl^- [22]. The results also revealed that the adsorption was not obviously affected between pH 2.5–4.0, and thereafter (pH > 4.0), the adsorption capacity of gold ions by OTPA-JS declined significantly. The maximum adsorption capacity occurred at pH 2.5 and 4.0 which was found to be consistent with the literatures [23–25]. In the acidic chloride solution (pH between 2.5 and 4), the maximum adsorption capacities were achieved due to the surface charge of the adsorbents and the existent state of Au(III) ion in the aqueous solutions. Many negatively charged chloro-anionic species of gold may be present in the solution, resulting in the greater electrostatic attraction between these species and protonated aminotrimethylenephosphonic acid groups of the adsorbent. However, on further increase of pH (>4.0) seems not to favor the gold adsorption. The reduction in adsorption capacity at higher pH values may be attributed to the reason as follows: increasing solution pH causes the hydrolysis reaction of $AuCl_4^-$ to proceed, and thus hydrolyzed chlorogold complexes appear in the aqueous chloride solution. The increasing OH^- in solution could compete with Cl^- and form hydroxo-containing gold complex. The hydroxo complex of gold in solution and deprotonation of organoptriphosphonic

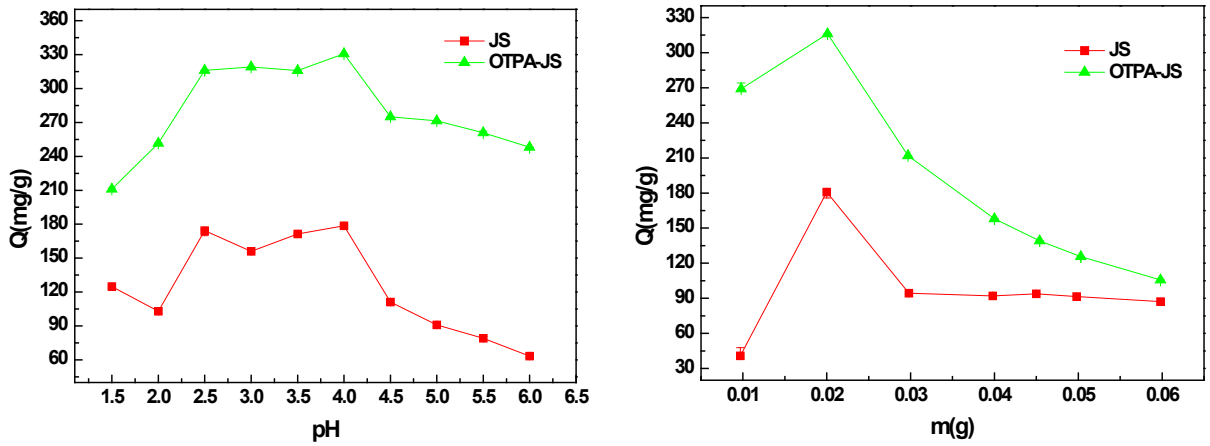

(1) (2)

Fig. 5. (1) Effect of pH on the adsorption for Au(III) on JS and OTPA-JS; (2) Effect of JS and OTPA-JS dosage on the adsorption for Au(III).

acid groups would lead to a decrease in electrostatic attractions between the negatively charged Au(III) anions and the positively charges adsorption sites of OTPA-JS. The pHs of real Au(III) samples/effluents from electroplating industrial wastewater are usually in the range of 2–3 [26,27], therefore, all the following experiments were performed at pH 2.5. The effect of pH for the unmodified adsorbent JS had the similar change trend,the adsorption capacity of JS for gold ions was 174.28 mg/g at pH 2.5, which was much lower than that of OTPA-JS (316.09 mg/g).

3.6. Effect of adsorbent dosage on gold adsorption

The effect of adsorbent dosage on the adsorption for Au(III) onto JS and OTPA-JS is illustrated in Fig. 5(2), the adsorption experiments were conducted in the adsorbent dosage range of 10.0–60.0 mg, it was clear that the adsorption capacities at the adsorption equilibrium increased and then decreased with the increase of adsorbent dosage, and the good adsorption capacities of the adsorbent for Au(III) exhibited with 20.0 mg of OTPA-JS. Though further increasing adsorbent dosage can be attributed to increased the biomass surface area and the availability of more adsorption sites. Nevertheless, the values of Au(III) uptake decreased with increasing the adsorbent dosage. The reason might be that higher biomass dosage could result in aggregates of functionalized adsorbent OTPA-JS, and might cause interference between binding sites at higher biomass dosage or insufficiency of metal ions in the solutions with respect to available binding sites. The adsorption capacity of JS (20.0 mg) was 180.74 mg/g, by contrast, that of OTPA-JS (20.0 mg) was 316.03 mg/g. It is evident that organotriphosphonic acid-modification benefited OTPA-JSA with a gold adsorption superior to JS.

3.7. Adsorption isotherms

The biosorption isotherms were characterized by definite parameters, whose values could express the surface properties and affinity of the biosorbent for metal ions, and the relationship between equilibrium adsorption capacity and equilibrium concentration at a certain temperature were studied. The adsorption isotherms of JS and OTPA-JSat different temperatures were studied and the results are shown in Fig. 6(1). The absorption capacities of JS and OTPA-JS for gold ions increased with the increase of temperature. At a certain temperature, it was explicit that the adsorption capacity of gold ions rose with the increase of the equilibrium concentration for unmodified japonica shells and organotriphosphonic acid-modified japonica shells. It is obvious that the adsorption capacities of OTPA-JS for gold ions were greater than those of JS over the whole concentration range.

To further understand the adsorption mechanism, in this study, three isotherm models were selected to fit the experimental data, namely the Langmuir, Freundlich and D-R isotherm models. The Langmuir model assumes that the uptake of metal ions occurs on a homogeneous surface by monolayer adsorption without any interaction between adsorbed ions. The Freundlich model assumes that the uptake or adsorption of metal ions occurs on a heterogeneous surface by monolayer adsorption [28]. In order to well understand the adsorption behaviors, we employed the Langmuir Eq. (6) and the Freundlich Eq. (7) (see Fig. 6(2) and Fig. 6(3)) to fit the experimental data, respectively [29,30]:

$$\frac{C_e}{q_e} = \frac{C_e}{q} + \frac{1}{qK_L} \tag{6}$$

$$\ln q_e = \ln K_F + \frac{\ln C_e}{n} \tag{7}$$

where q_e is the equilibrium metal ion concentration on the adsorbent, mg/g; C_e is the equilibrium concentration of gold ions, mg/L, q is the saturated adsorption capacity, mg/g; K_L is the Langmuir constant, L/mg; n is the Freundlich constant and K_F is the binding energy constant

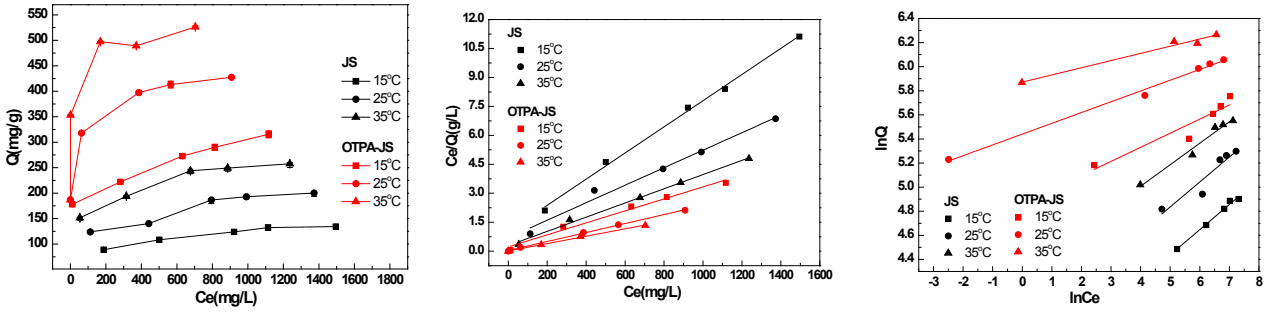

(1) (2) (3)

Fig. 6. (1) The isothermal adsorption of the agricultural waste-based adsorbent JS and OTPA-JS for Au(III) at different temperatures; (2) The Langmuir isotherms of the adsorbent JS and OTPA-JS for Au(III) at different temperatures; (3) The Freundich isotherms of the adsorbent JS and OTPA-JS for Au(III) at different temperatures..

Table 2
Isotherm parameters of the Langmuir, Freundlich and Dubinin-Radushkevich models for the adsorption for gold ions onto JS and OTPA-JS

Adsorbents	T (°C)	Langmuir			Freundlich			Dubinin-Radushkevich			
		q (mg/g)	K_L (L/mg)	R^2	K_F (mg/g)	n	R^2	$\ln q_{max}$ (mol/g)	β×10⁸ (mol²/ J²)	E (kJ/mol)	R^2
JS	15	147.71	0.0066	0.9965	29.76	4.7840	0.9874	−6.86	−3.07	12.76	0.9871
	25	220.75	0.0065	0.9796	44.65	4.8230	0.8639	−6.51	−2.66	13.71	0.8332
	35	271.74	0.0126	0.9943	73.24	5.6026	0.9673	−6.30	−2.02	15.73	0.9523
OTPA-JS	15	322.58	0.0137	0.9801	129.37	8.5463	0.8666	−6.32	−1.31	19.54	0.8118
	25	431.03	0.0604	0.9983	230.47	11.17	0.9916	−6.05	−0.70	26.73	0.9635
	35	523.56	0.1713	0.9979	354.92	16.79	0.9689	−5.84	−0.50	31.62	0.9752

reflecting the affinity of the adsorbents to metal ions, mg/g. The parameters for the isotherms obtained from Fig. 6(2) and Fig. 6(3) are presented in Table 2. To quantify the prediction of isotherm constants more directly, the deviation of the fitted values and the experimental values for the Langmuir (a) and Freundlich (b) isotherms was plotted as shown in Fig. S1 (available online in the supplemental materials). The profile indicated that the predictions of the Langmuir isotherm were closer to the measured equilibrium values than those of the Freundlich isotherm for the entire range of concentrations and temperatures, especially for the adsorbent OTPA-JS. For the Langmuir isotherm, the range of the magnitude or variation of derivation (error) of OTPA-JS (0.085 mg/g^{-1}–0.039 mg/g) was smaller generally than that of JS (0.38 mg/g^{-1}–0.17 mg/g). Moreover, the data fitting of the adsorption equilibrium for gold ions by OTPA-JS at 25°C was presented in Table S3 (available online in the supplemental materials). Just as mentioned in Ref [31], the related procedure to estimate parameters utilized the concept of minimizing the objective function. To estimate the isotherm constants, sum of absolute error (SAE), average relative error (ARE), and sum of the square of error (SSE) were used as objective function, respectively, which were minimized. The equilibrium values predicted from the isotherms are termed as linear transformed method, denoted as LTFM [31]. The optimum (minimum) of error function yielded minimum standard deviation and minimum variance of error, thus offering the optimal values of the parameters that underlined the characteristics of the isotherms. As seen from Table 2 and Table S3, the R^2 values obtained from the Langmuir model are much closer to 1 than those from the Freundlich model, suggesting the Langmuir model are better than the Freundlich model to fit the adsorption isotherms of JS and OTPA-JS for Au(III), and the fitting results of the Langmuir isotherm provided better predictions and closer to experimental values. The Langmuir model assumes the adsorbent has a finite number of binding sites with all sites having the same binding power and the adsorption of each site is independent of each other. As a result, the adsorption of JS and OTPA-JS for gold ions was attributed to monolayer adsorption, monolayer complexation between gold ions and the adsorption substrate is the dominant coverage in these samples. The maximum adsorption capacity of JS and OTPA-JS obtained by Langmuir isotherm for Au(III) adsorption was 271.74 mg/g and 523.56 mg/g at 35°C, respectively. It was clear that the adsorption capacity of OTPA-JS was more higher than that of JS, in addition, it was relatively high when compared with several other adsorbents such as L-lysine modified crosslinked chitosan resin, thiol cotton fiber, alfalfa biomass, etc [32–36]. The above-mentioned research results show that the agricultural waste-based adsorbent organotriphosphonic acid-modified japonica shell isvery useful for the bioremoval of gold ions.

The equilibrium data were also subjected to the D-R isotherm model to determine the nature of adsorption process. The D-R isotherm equation [37] is:

$$\ln q_e = \ln q_{\max} - \beta\varepsilon^2 \tag{8}$$

where q_e is the amount of metal ions adsorbed on per unit weight of adsorbent, mol/g; q_{max} is the maximum adsorption capacity, mol/g; β is the activity coefficient related to adsorption mean free energy, mol^2/J^2; ε is the Polanyi potential (ε = RT ln(1 + 1/C_e)). The values of mean free energy (E, kJ/mol) can be calculated by using β values:

$$E = \frac{1}{\sqrt{-2\beta}} \tag{9}$$

It is known that magnitude of apparent adsorption energy E is useful for estimating the type of adsorption and if this value is below 8 kJ/mol the adsorption type can be explained by physical adsorption, between 8 and 16 kJ/mol the adsorption type can be explained by ion exchange, and over 16 kJ/mol the adsorption type can be explained by a stronger chemical adsorption than ion exchange [38]. The results of the D-R adsorption isotherm for Au(III) from simulated wastewater onto JS and OTPA-JS are shown in Fig. 7(1) and Fig. 7(2) and Table 2. The data in Table 2 displayed that the E values of JS at different temperatures were between 8 kJ/mol and 16 kJ/mol, however, those E values of OTPA-JS were greater than 16 kJ/mol, indicating that the adsorption processes of gold ions onto OTPA-JS in aqueous solutions was carried out by chemical adsorption mechanism, which implied that this adsorption mechanism was different from ion exchange mechanism for the adsorbent JS.

3.8 Adsorption kinetics

Kinetics involves the study of the rates of chemical process and facilitates an understanding of the factors that affect those rates. The study of chemical kinetics includes careful monitoring of the experimental conditions that influence the speed of a chemical reaction in its race toward equilibrium. These investigations could provide information about the possible adsorption mechanisms and the data obtained is used to develop appropriate models to describe the interactions. The adsorption kinetics of OTPA-JS for Au(III) were investigated at 15–35°C to determine the adsorption equilibrium time, and the results are shown in Fig. 8(1). It was clear that from the figure that the adsorption capacities of OTPA-JS for Au(III) increased with the extension of contact time, it was obvious that in the first 120 min, the adsorption was rapid, and then slowed considerably. The reason perhaps is that, Au(III) ions might enter easily the accessible pore sites and bind with the chelating ligands in initial fast adsorption step. While in the slow adsorption step, some gold ions might be hampered to diffusion into the deeper pores. As a significant practical importance, the rapid kinetics will facilitate smaller reactor volumes ensuring efficiency and economy. It could be observed that the modified japonica shells required 14 h to reach adsorption equilibrium. Thus its excellent adsorption capacity for Au(III) was 357.89 mg/g when the initial solution concentration was 2.43 mmol/L at 35°C.

The adsorption procedure of adsorbents for metal ions is generally considered to take place through two mechanisms of film diffusion and particle diffusion. In order to distinguish film diffusion from particle diffusion controlled adsorption, the kinetics experimental results were usually analyzed by the Boyd equation and the Reichenberg equation [39–41]. The relevant equations are given as follows:

$$F = 1 - \frac{6}{\pi^2}\sum_{n-1}^{\infty}\frac{1}{n^2}\left[\frac{-D_i t\pi^2 n^2}{r_0^2}\right] \tag{10}$$

$$\text{or } F = 1 - \frac{6}{\pi^2}\sum_{n-1}^{\infty}\frac{1}{n^2}\exp\left[-n^2 Bt\right] \tag{11}$$

where n is an integer that defines the infinite series solution; D_i is the effective diffusion coefficient of metal ions in the adsorbent phase; r_0 is the radius of the adsorbent particle,

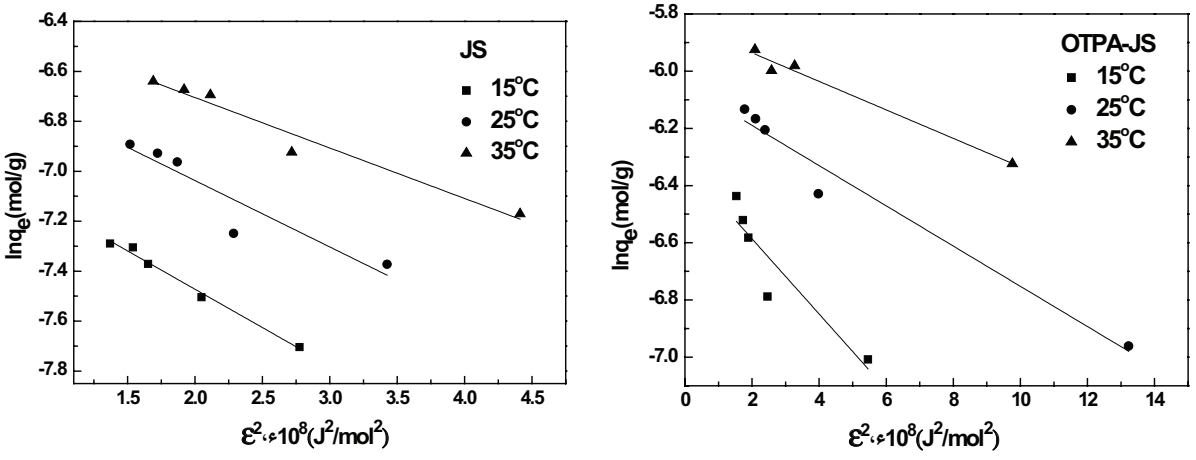

(1) (2)

Fig. 7. The Dubinin-Radushkevich isotherms of JS (1) and OTPA-JS (2) for gold ions at different temperatures.

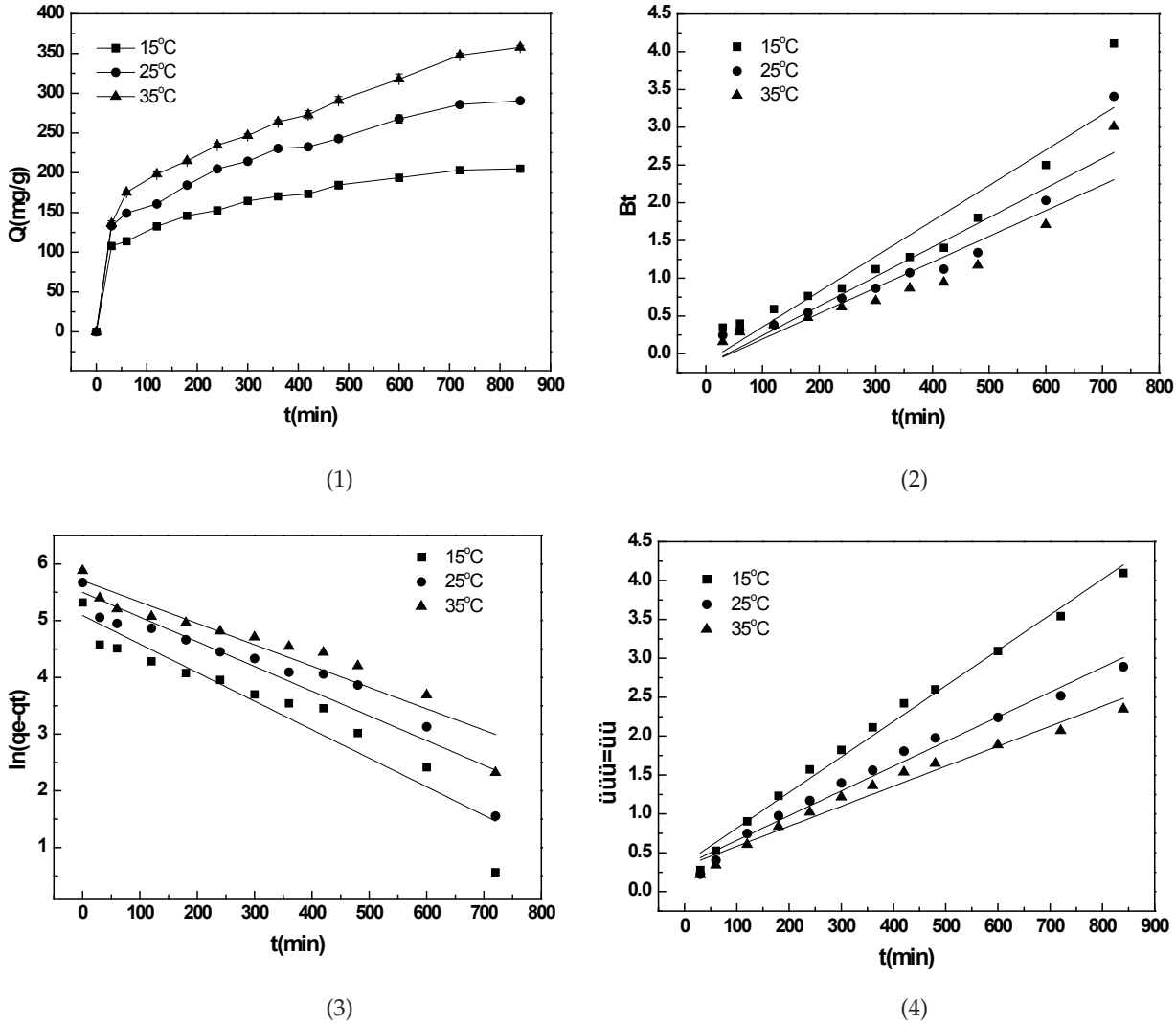

Fig. 8. (1) Adsorption kinetics of Au(III) on OTPA-JS at different temperatures; (2) *Bt* versus time plots for OTPA-JS at different temperatures; (3) Pseudo-first-order kinetic plots for the adsorption of Au(III) onto OTPA-JS at different temperatures; (4) Pseudo-second-order kinetic plots for the adsorption of Au(III) onto OTPA-JS at different temperatures.

assumed to be spherical; *F* is the fractional attainment of equilibrium at time *t* and is obtained by the expression:

$$F = \frac{q_t}{q_0} \tag{12}$$

where q_t is the amount of adsorbate taken up at time *t* and q_0 is the maximum equilibrium uptake.

$$B = \frac{\pi^2 D_i}{r_0^2} = \text{ time constant} \tag{13}$$

Values of *Bt* were obtained from corresponding values of F. *Bt* values for each F were given by Reichenberg and the results are plotted in Fig. 8(2), and Bt–F fitting results are shown in Table 3. Plots of *Bt* versus time of gold ions adsorption onto OTPA-JS at 15–35°C were employed to distinguish between the film diffusion and particle diffusion controlled adsorption. If the plots were straight line passing through the origin, the adsorption process should be governed by the particle diffusion mechanism, otherwise, it might be dominated by the film diffusion. As shown in Fig. 8(2), the lines of *Bt* versus time plots did not pass through the origin in the cases studied, demonstrating the film diffusion, not the particle diffusion, dominated the adsorption processes of OTPA-JS for Au(III) from simulated wastewater solutions.

Table 3
The linear equations of *Bt* versus time and the coefficients R^2

T(°C)	Linear equation	R^2
15	Bt = 0.00469t – 0.11529	0.8737
25	Bt = 0.00391t – 0.15097	0.8624
35	Bt = 0.00341t – 0.14738	0.8444

The pseudo-first-order and pseudo-second-order models are usually used to test the experimental data and thus

express the adsorption kinetic process [42,43], and they can be expressed by Eqs. (14) and (15), respectively:

$$\ln\left(q_e - q_t\right) = \ln q_e - k_1 t \tag{14}$$

$$\frac{t}{q_t} = \frac{1}{k_2 q_e^2} + \frac{t}{q_e} \tag{15}$$

where q_e is the amount of metal adsorbed at equilibrium per unit weight of adsorbent, mg/g, q_t is the amount of metal ion adsorbed at t time, mg/g, k_1 (min^{-1}) and k_2 (g/mg min) are the rate constants of pseudo-first-order and pseudo-second-order adsorption. The experimental and calculated q_e values, k_1, k_2 and regression coefficient (R_2) values obtained from pseudo-first-order and pseudo-second-order kinetic models are shown in Table 3.

The pseudo-first-order kinetic and pseudo-second-order kinetic plots and kinetic parameters for the adsorption of gold ions onto OTPA-JS at different temperatures are shown in Fig. 8(3) and Fig. 8(4), respectively. As can be seen from Table 4, the obtained coefficients values of the pseudo-second-order model (>0.9595) were better than those of the pseudo-first-order model for the adsorbent (0.8819–0.8886), suggesting the pseudo-second-order model was more suitable to describe the adsorption kinetics of OTPA-JS for Au(III). Moreover, the calculated q_e values depending on the pseudo-second-order model were much closer to the experimental values q_e(exp). Therefore, the adsorption kinetics could well be approximated more favorably by the pseudo-second-order kinetic model for gold ions from aqueous solutions onto OTPA-JS. Based on the kinetics analyses, it is clear that the introduction of organoptriphosphonic acid functional groups onto japonica shells has greatly enhanced the effective removal rate of gold ions.

The magnitude of activation energy (*Ea*) can provide information about whether the adsorption process is physical or chemical. The activation energy of the adsorption process was calculated by the Arrehenius Eq. (16):

$$\ln k = -\frac{Ea}{RT} + \ln A \tag{16}$$

where k is the pseudo-second-order rate constant of sorption (g/mg·min), A is the Arrhenius constant which is a temperature independent factor (g/mg·min), *Ea* is the activation energy of sorption (kJ/mol), R is the gas constant (8.314 J/mol K) and T is the absolute temperature (K). A straight line with slope $-Ea/R$ of ln k vs. $1/T$ is obtained (Fig. S2, available online in the supplemental materials). The obtained activation energy value for OTPA-JS was –38.82 kJ/mol, which was greater than that of *Ea* (16.29 kJ/mol) reported by Fujiwara et al. [32]. The requirements of the physical adsorption activation energy are relatively small, generally not more than 4.2 kJ/mol. However, chemical adsorption is specific, and the forces are much stronger than in physical adsorption [44]. Therefore, the result suggests that the adsorption of Au(III) on OTPA-JS is chemical adsorption.

3.9. Determination of the thermodynamics parameters

Thermodynamic parameters were evaluated to confirm the nature of the adsorption of gold ionsby OTPA-JS. The thermodynamic parameters including the Gibbs free energy (ΔG), enthalpy change (ΔH) and entropy change (ΔS) were calculated to evaluate the thermodynamic feasibility and spontaneous nature of the process. They were determined using the following equations [32,45]:

$$K_c = \frac{C_{Ae}}{C_e} \tag{17}$$

$$\log K_c = \frac{\Delta S}{2.303R} - \frac{\Delta H}{2.303RT} \tag{18}$$

$$\Delta G = -RT \ln K_c \tag{19}$$

where C_e and C_{Ae} are the equilibrium concentration in solution (mg/L) and the solid phase concentration at equilibrium (mg/L), respectively. K_c is the partition coefficients of each temperature. R is the gas constant (8.314 J/mol K), and T is the temperature in Kelvin. Using the above relationships, the thermodynamic parameters, including the standard free energy change (ΔG), enthalpy change (ΔH) and entropy change (ΔS), were calculated from the variation of the thermodynamic equilibrium constant K_c with respect to temperature. As shown in Fig. S3 (available in the Supplemental Material), from the slope and y-intercept of the linear plot of ln K_c versus $1/T$, the changes of enthalpy and entropy could be obtained. The thermodynamic parameters were listed in Table 4. The adsorption thermodynamic parameters ΔG, ΔH and ΔS

Table 5
The thermodynamic parameters of OTPA-JS for Au(III)

T (°C)	ΔG (kJ/mol)	ΔH (kJ/mol)	ΔS (J/K· mol)
15	–96.33	96.87	334.81
25	–99.68		
35	–103.02		

Table 4
The adsorption kinetic parameters of OTPA-JS for Au(III)

T (°C)	q_e(exp) (mg/g)	Pseudo-first-order kinetics			Pseudo-second-order kinetics		
		K_1 (min^{-1})	q_e(cal) (mg/g)	R_1^2	K_2*10^{-3} (g/mg·min)	q_e (cal) (mg/g)	R_2^2
15	205.01	0.0050	162.65	0.8883	0.0580	218.82	0.9926
25	290.57	0.0044	244.58	0.8819	0.0296	314.47	0.9595
35	357.89	0.0038	300.74	0.8886	0.0203	389.11	0.9841

were –103.02 kJ mol^{-1} (35°C), 96.87 kJ mol^{-1}, and 334.81 J K^{-1} mol^{-1}, respectively (Table 5). The positive value of ΔH reflected an endothermic nature of gold adsorption onto OTPA-JS and indicated that the adsorption was favored at high temperature, which was supported by the increase of gold adsorption onto OTPA-JS with rising temperature. ΔH of chemical adsorption is larger than 40 kJ/mol, therefore, the adsorption of gold ions onto OTPA-JS could be regarded as a chemisorption process. The positive ΔS suggested increased randomness at the solid/solution interface during the adsorption of gold ions from simulated wastewater onto OTPA-JS. The negative value of ΔG for gold ions adsorption on OTPA-JS indicated that the adsorption process was spontaneous. The values of ΔG became more negative with increasing temperature, as the temperature increased, the absolute values of ΔG increased accordingly, which indicated that the adsorption process was more favorable at high temperature. A more negative data of ΔG implies a greater driving force of adsorption, resulting in a higher adsorption capacity. The adsorption on solids is classified into physical adsorption and chemical adsorption, however, the dividing line between them is not very clear. Physical adsorption is nonspecific, and the variation of energy for physical adsorption is usually substantially smaller than that of chemical adsorption, which are highly specific. Generally, the data ΔG for physisorption are between –20 and 0 kJ/mol and for chemisorption is between –80 and –400 kJ/mol [46]. When the temperature increased from 15 to 35°C for gold adsorption onto OTPA-JS, ΔG increased from –96.33 to –103.02 kJ/mol. This can be considered as chemical adsorption and more favorable at high temperature. Therefore, the thermodynamics results implied the chemisorption might dominate the adsorption of gold ion onto OTPA-JS. The thermodynamic data were in good agreement with chemical adsorption mechanism derived by the above mentioned results of D-R isotherm and the activation energy value of the gold ions adsorption process.

3.10. Adsorption mechanism of Au(III) ions on OTPA-JS

D-R isotherm and thermodynamic study, the obtained activation energy value for OTPA-JS indicated that the process was chemical in nature. In order to make the gold adsorption process clear, furthermore, some methods of analysis have been used to study the corresponding adsorption mechanism. Fig. 9 (1) shows the FTIR spectra of unloaded and Au-loaded OTPA-JS. A strong adsorption peak was observed for both unloaded and Au-loaded OTPA-JS at 3435 cm^{-1}, which may be assigned to OH stretching vibration in hydroxyl groups. There was an obvious reduction in the hydroxyl stretching band, in addition, the band at 2841 cm^{-1} assigned to (P)-O-H stretching vibration before adsorption was obviously weakened after adsorption, which was associated with the interactions between the phosphonic acid groups on OTPA-JS with gold ions. Some other peaks, which may attributed to certain functional groups were shifted the adsorption, signifying the feasible participation of the functional groups on the surface of OTPA-JS. For example, the –CH_2- symmetric stretching at 2920 shifted to 2929 cm^{-1}. The results further confirmed the complexation of organophosphonic acid and gold ions during the heavy metals removal process. The XPS of OTPA-JS-Au is shown in Fig. 9(2), and it could be seen that the binding energies of Au4f5/2 and Au4f7/2 were 87.317 and 83.707 eV, respectively. Compared with the standard binding energy, the binding energy of Au4f5/2 has shifted to the low energy direction, and the binding energy of Au4f7/2 has shifted to the high energy direction to some extent, which indicated that there were the interactions between gold and the surface molecules of the adsorbent OTPA-JS. The SEM image of OTPA-JS after adsorption is shown in Fig. 9(3). Obviously, there were a number of elemental gold distributed on the surface of OTPA-JS after adsorption. It was probably because that Au(III) ions were reduced to Au(0) after adsorption since organophosphonic acid has reducibility and the corresponding in situ reduction reaction was carried out. The generation of Au(0) on OTPA-JS after the adsorption was elucidated by XRD patterns shown in Fig. 9(4). These particles were proved to be metallic gold since the characteristic peaks of gold at 2θ = 38.0°, 44.1°, and 64.3° appeared in the X-ray diffraction pattern of OTPA-JS-Au, which certainly belonged to elemental gold verifying the reduction of Au(III) to Au(0) [25]. This suggested Au(III) underwent subsequent reduction after being adsorbed onto OTPA-JS surface. Therefore, the initial chemisorptions of Au(III) ions by OTPA-JS, which were dominated by electrostatic attraction and chelation, were followed by simultaneous reduction to metallic gold form, and the schematic representation of the process and predicted adsorption mechanism is shown in Fig. 10. In the present process, conversion of gold ions to metallic gold was achieved without use of any external reducing agents.

3.11. Applications of OTPA-JS for adsorption of gold/copper ions from gold-plating wastewater

The adsorption abilities of OTPA-JS have also been investigated in the industrial wastewater systems (sample 1 and sample 2). The adsorption kinetics results of Au(III) and Cu(II) onto OTPA-JS from sample 1 and sample 2 at ambient temperature are shown in Fig. 11(1) and Fig. 11(4), respectively. It was clear that the adsorption capacities of OTPA-JS for Au(III) increased with the extension of contact time, the adsorption was rapid in the first 360 min and 240 min for sample 1 and sample 2, respectively, and then slowed considerably. However, the adsorption capacities of OTPA-JS for Cu(II) kept low during the whole adsorption process. It followed the order of Au(III) > Cu(II), which is in the order of increasing ionic radius of the metal ions studied. The greater the ionic radius, the smaller is the hydrated ionic radius and greater is the affinity of the heavy metal ions on the active sites of the adsorbent. The pseudo-first-order kinetic and pseudo-second-order kinetic plots and kinetic parameters for the adsorption of Au(III) and Cu(II) onto OTPA-JS at room temperature are shown in Figs. 11(2), 11(3), 11(5), 11(6) and Table 6. As can be seen from Table 6, the obtained coefficients values of the pseudo-second-order model (>0.9431) were better than those of the pseudo-first-order model for the adsorbent (0.8401–0.8976), suggesting the pseudo-second-order model was more suitable to describe the adsorption kinetics of OTPA-JS for Au(III) and Cu(II) in gold-plating wastewater. This reveals that the rate limiting step may be

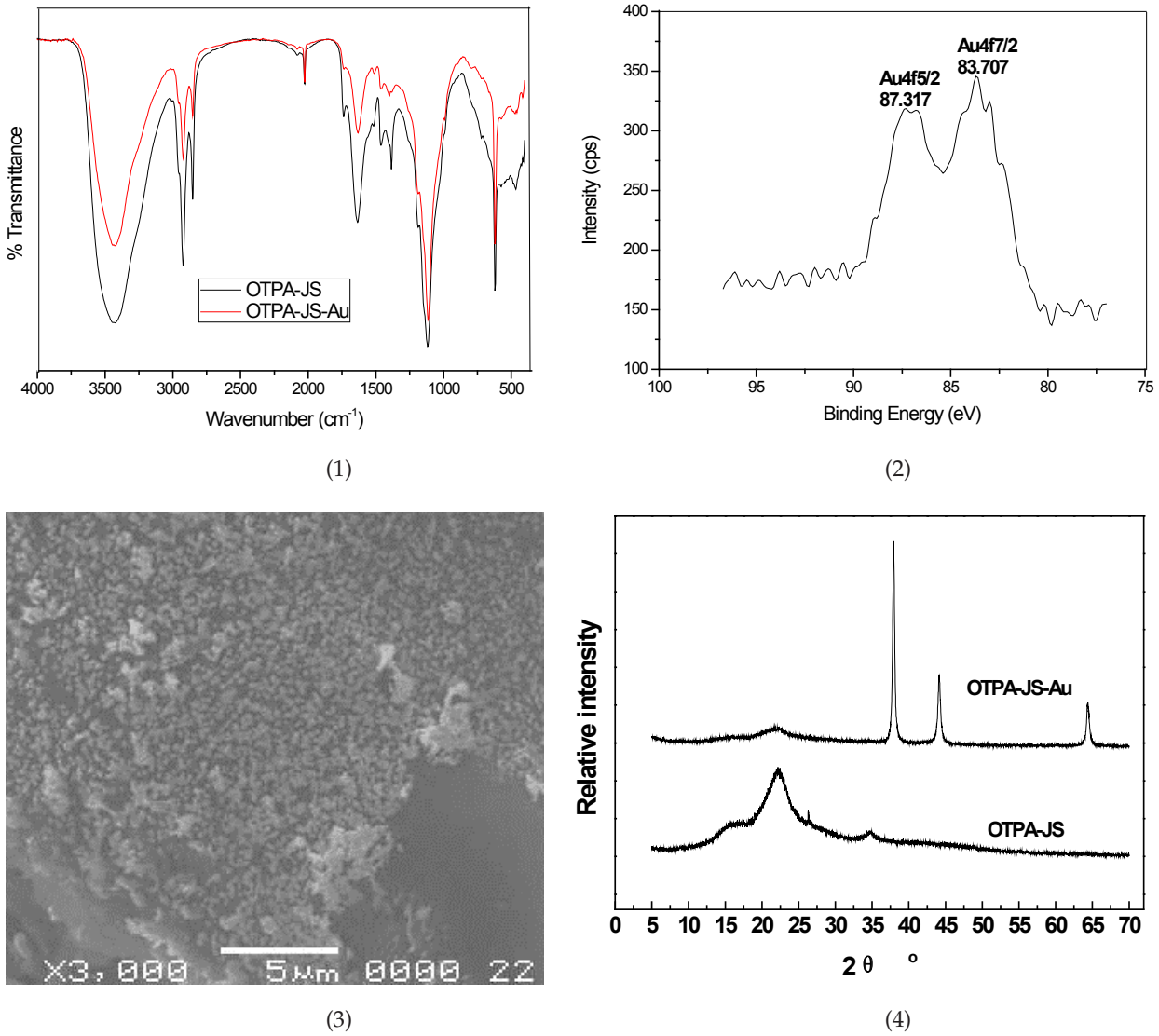

Fig. 9. (1) FT-IR spectra of OTPA-JS and OTPA-JS-Au; (2) X-ray photoelectron spectra of OTPA-JS-Au; (3) SEM image of OTPA-JS-Au; (4) XRD patterns of OTPA-JS and OTPA-JS-Au.

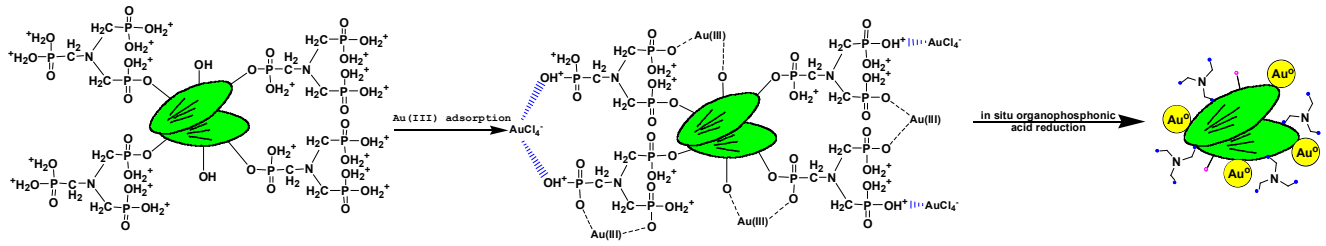

Fig. 10. Schematic diagram of gold adsorption mechanism by OTPA-JS.

chemical adsorption involving valence forces through sharing or exchange of electrons between OTPA-JS and metal ions, and in situ reduction reaction. The high affinity of the agricultural waste-based adsorbent OTPA-JS toward gold ion binding at low pH and ambient temperature will work well in the conditions of industrial waste effluents.

4. Conclusions

In this work, the feasibility of using a organotriphosphonic acid modified japonica shells for adsorption of gold ions from wastewater has been investigated. Organotriphosphonic acid functional groups have been successfully

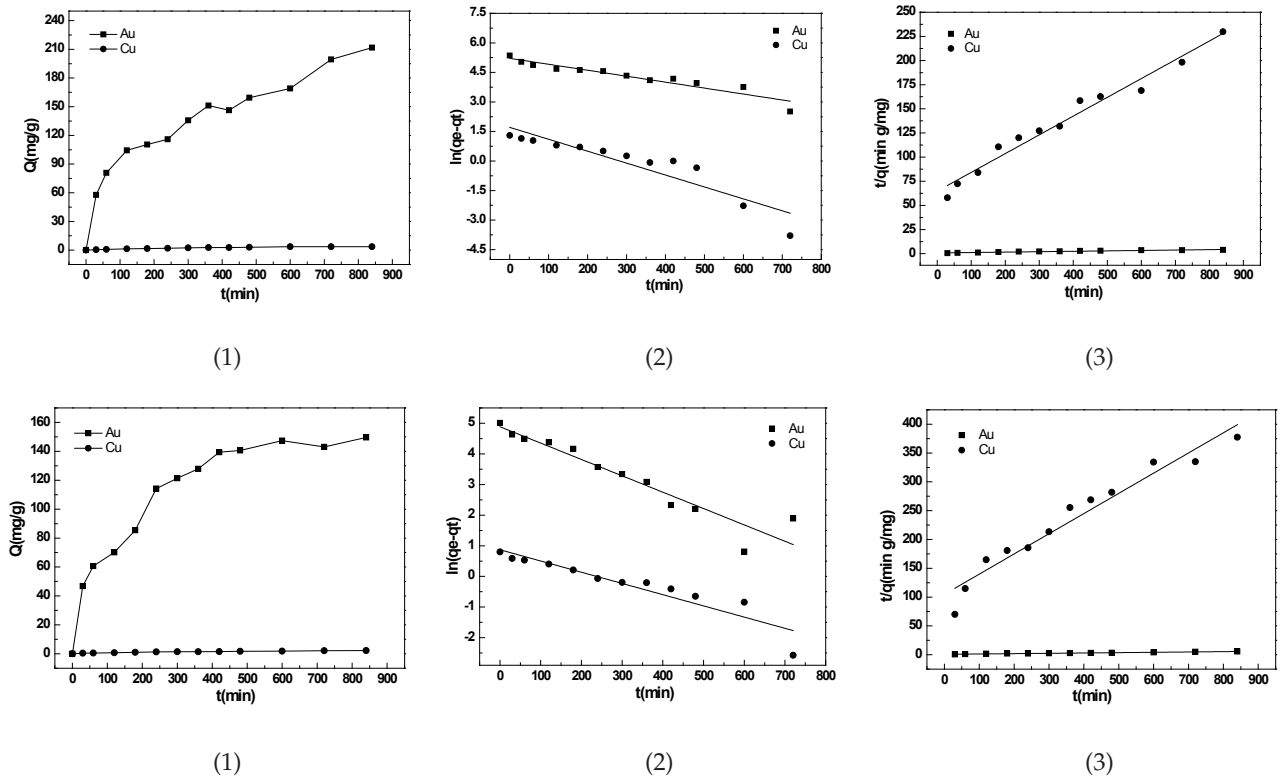

Fig. 11. The adsorption kinetics of Au(III) and Cu(II) onto OTPA-JS from the sample 1 (1) and the sample 2 (4); Pseudo-first-order kinetic plots for the adsorption of Au(III) and Cu(II) onto OTPA-JS from the sample 1 (2) and the sample 2 (5); Pseudo-second-order kinetic plots for the adsorption of Au(III) and Cu(II) onto OTPA-JS from the sample 1 (3) and the sample 2 (6).

Table 6
Kinetic parameters of the adsorption of Au(III) and Cu(II) onto OTPA-JS from the sample 1 and the sample 2 from industrial gold-plating wastewater

Samples	Ions	q_e(exp) (mg/g)	Pseudo-first-order kinetics			Pseudo-second-order kinetics		
			K_1 (min^{-1})	q_e(cal) (mg/g)	R_1^2	K_2*10^{-3} (g/mg·min)	q_e (cal) (mg/g)	R_2^2
1	Au(III)	211.74	0.0030	183.88	0.8920	0.0241	233.64	0.9432
	Cu(II)	3.66	0.0061	5.53	0.8401	0.5822	5.15	0.9702
2	Au(III)	149.63	0.0053	132.42	0.8976	0.0453	173.01	0.9852
	Cu(II)	2.23	0.0037	2.39	0.8627	1.1717	2.85	0.9431

introduced on the surface of japonica shells, which greatly enhanced their adsorption for heavy metals ions, especially for gold ions. The adsorption selectivity showed that OTPA-JS displayed strong affinity for gold in the aqueous solutions and exhibited 100% selectivity for gold ions in the presence of Co(II), Zn(II), Cr(III) and Cd(II).The investigation indicated the best interpretation for the experimental data was given by the Langmuir isotherm equation, the maximum adsorption capacities of JS and OTPA-JS at 35°C were 271.74 and 523.56 mg/g, respectively. The adsorption kinetics of OTPA-JS can be modeled by pseudo second-order rate equation wonderfully, the activation energy value for Au(III) onto OTPA-JS was –38.82 kJ/mol and the adsorption thermodynamic parameters ΔG, ΔH and ΔS were –103.03 kJ·mol^{-1}, 96.87 kJ·mol^{-1}, and 334.82 J· K^{-1}·mol^{-1}, respectively. The adsorption mechanism was elucidated as the electrostatic attraction/chelation – in situ organotriphosphonic acid reduction mechanism, and conversion of gold ions to metallic gold was achieved without use of any external reducing agents. The applications of OTPA-JS for Adsorption of gold/copper ions from gold-plating wastewater were also carried out. From the practical point of view, the high adsorption capacity and good adsorption selectivity make the organotriphosphonated japonica shells have a significant potential for uptaking specious metal ions from industrial wastewater using adsorption method.

Acknowledgement

The support provided by the National Natural Science Foundation of China (No. 51673090, 51173074, and

51102127), the Science and Technology Development Plan from Shandong Provincial Education Department (NO. J17KA006), and the Natural Science Foundation of Shandong Province (No. ZR2017PB006) is greatly appreciated.

References

[1] E. Vences-Alvarez, E. Razo-Flores, I. Lazaro, R. Briones-Gallardo, G. Velasco-Martinez, R. Rangel-Mendez, Gold recovery from dilute solutions from a mine in closing process: Adsorption-desorption onto carbon materials, J. Mol. Liq., 240 (2017) 549–555.

[2] M.W. Yap, N.M. Mubarak, J.N. Sahu, E.C. Abdullah, Microwave induced synthesis of magnetic biochar from agricultural biomass for removal of lead and cadmium from wastewater, J. Ind. Eng. Chem., 45 (2017) 287–295.

[3] R.K. Thines, N.M. Mubarak, S. Nizamuddin, J.N. Sahu, E.C. Abdullah, P. Ganesan, Application potential of carbon nanomaterials in water and wastewater treatment: A review, J. Taiwan Inst. Chem. E., 72 (2017) 116–133.

[4] N.M. Mubarak, A. Faghihzadeh, K.W. Tan, J.N. Sahu, E.C. Abdullah, N.S. Javakumar, Microwave assisted carbon nanofibers for removal of zinc and copper from waste water, J. Nanosci. Nanotechnol., 16(3) (2017) 1847–1856.

[5] J.N. Sahu, J. Acharya, B.K. Sahoo, B.C. Meikap, Optimization of lead (II) sorption potential using developed activated carbon from tamarind wood with chemical activation by zinc chloride, Desal. Water Treat., 57(5) (2016) 2006–2017.

[6] N.M. Mubarak, M. Thobashinni, E.C. Abdullah, J.N. Sahu, Comparative kinetic study of removal of Pb^{2+} ions and Cr^{3+} ions from waste water using carbon nanotubes produced using microwave heating, C J. Carbon Res., 2(7) (2016) 1–16.

[7] Y. Tian, P. Yin, R. Qu, C. Wang, H. Zheng, Z. Yu, Removal of transition metal ions from aqueous solutions by adsorption using a novel hybrid material silica gel chemically modified by triethylenetetraminomethylenephosphonic acid, Chem. Eng. J., 162 (2010) 573–579.

[8] N.V. Nguyen, J. Lee, S. Kim, M.K. Jha, K. Chung, J. Jeoong, Adsorption of gold(III) from waste rinse water of semiconductor manufacturing industries using Amberlite XDA-7HP resin, Gold Bull., 43 (2010) 200–208.

[9] A. Mourpichai, T. Jintakosol, W. Nitayaphat, Adsorption of gold ion from a solution using montmorillonite/alginate composite, Mater. Today: Proc., 5 (2018) 14786–14792.

[10] M. Xu, P Yin, X. Liu, X. Dong, Y. Yang, Z. Wang, R. Qu, Optimization of biosorption parameters of Hg(II) from aqueous solutions by the buckwheat hulls using respond surface methodology, Desal. Water Treat., 51 (2013) 4546–4555.

[11] B.C. Choudhary, D. Paul, A.U. Borse, D.J. Garole, Surface functionized biomass for adsorption and recovery of gold from electronic scrap and refinery wastewater, Sep. Purif. Technol., 195 (2018) 260–270.

[12] T. Mao, X. Li, S.K. Jiang, L. Tang, J.Y. Wang, H. Xu, Z.J. Xu, Discussion on strategy of grain quality for super high yielding japonica rice in Northwest China, J. Interg. Agric., 16 (2017) 60345–60347.

[13] E.J. Siqueira, I.V.P. Yoshida, L.C. Pardini, M.A. Schiavon, Preparation and characterization of ceramic composites derived from rice husk ash and polysiloxane, Ceram. Int., 35 (2009) 213–220.

[14] T. Torres-Blancas, G. Roa-Morales, C. Fall, C. Barrera-Díaz, F. Ureña-Nuñez, T.B.P. Silva, Improving lead sorption through chemical modification of de-oiled allspice husk by xanthate, Fuel, 110 (2013) 4–11.

[15] M.J. Frisch, G.W. Trucks, H.B. Schlegel, Gaussian 03, Gaussian, Inc, Pittsburgh PA (2003).

[16] J. Li, L. Meng, Z. Sun, Z. Liu, Y. Zhao, J. Zhang, Y. Zhu, X. Lu, L. Liu, N. Zhang, Synthesis, crystal structure and characterizations of a new 3D porous zinc phosphonate: $Zn_6[(O_3PCH_2)_2NHC_6H_{11}]_4 \cdot 6H_2O$, Inorg. Chem. Commun., 11 (2008) 211–214.

[17] L. Jing, Y. Zhang, X. Li, X. He, L. Yang, Zirconium phosphonate doped PVA/chitosan hybrid gel beads for enhanced selective extraction of Pb^{2+} from water, J. Taiwan Inst. Chem. Eng., 56 (2015) 103–112.

[18] J.O. Joswig, S. Hazebroucq, G. Seifert, Properties of the phosphonic-acid molecule and the proton transfer in the phosphonic-acid dimer, J. Mol. Struc. Theochem., 816 (2007) 119–123.

[19] M. Sawicka, P. Storoniak, P. Skurski, J. Blazejowski, J. Rak, TG-FTIR, DSC and quantum chemical studies of the thermal decomposition of quaternary methylammonium halides, Chem. Phys., 324 (2006) 425–437.

[20] E.G. Robertson, IR-UV ion-dip spectroscopy of N-phenyl formamide, and its hydrated clusters, Chem. Phys. Lett., 325 (2000) 299–307.

[21] T. Ogata, Y. Nakano, Mechanisms of gold recovery from aqueous solutions using a novel tannin gel adsorbent synthesized from natural condensed tannin, Water Res., 39 (2005) 4281–4286.

[22] Y.C. Chang, D.H. Chen, Recovery of gold(III) ions by a chitosan-coated magnetic nano-adsorbent, Gold Bull., 39 (2006) 98–102.

[23] R. Qu, C. Sun, M. Wang, C. Ji, Q. Xu, Y. Zhang, C. Wang, H. Chen, P. Yin, Adsorption of Au(III) from aqueous solution using cotton fiber/chitosan composite adsorbents, Hydrometallurgy, 100 (2009) 65–71.

[24] M.E.H. Ahamed, X.Y. Mbianda, A.F. Mulaba-Bafubiandi, L. Marjanovic, Selective extraction of gold(III) from metal chloride mixtures using ethylenediamine N-(2-(1-imidazoly)ethyl) chitosan ion-imprinted polymer, Hydrometallurgy, 140 (2013) 1–13.

[25] M.A.Z. Abidin, A.A. Jalil, S. Triwahyono, S. Hazirah Adam, N.H. Nazirah Kamarudin, Recovery of gold(III) from an aqueous solution onto a durio zibethinus husk, Biochem. Eng. J., 54 (2011) 124–131.

[26] S. Ishikawa, K. Suyama, K. Arihara, M. Itoh, Uptake and recovery of gold ions from electroplating wastes using eggshell membrane, Bioresour. Technol., 81 (2002) 201–206.

[27] M. Soleimani, T. Kaghazchi, Adsorption of gold ions from industrial wastewater using activated carbon derived from hard shell of apricot stones – An agricultural waste, Bioresour. Technol., 99 (2008) 5374–5383.

[28] Y.S. Ho, Selection of optimum sorption isotherm, Carbon, 42 (2004) 2115–2116.

[29] I. Langmuir, The adsorption of gases on plane surfaces of glass, mica and platinum, J. Am. Chem. Soc., 57 (1918) 1361–1403.

[30] H. Freundlich, Uber die adsorption in losungen, Z. Phys. Chem., 57 (1906) 385–470.

[31] R.R. Karri, J.N. Sahu, N.S. Jayakumar, Optimal isotherm paprameter for phenol from aqueous solutions onto coconut shell based activated carbon: error analysis of linear and non-linear methods, J. Taiwan Inst. Chem. Eng., 80 (2017) 472–487.

[32] K. Fujiwara, A. Ramesh, T. Maki, H. Hasegawa, K. Ueda, Adsorption of platinum (IV), palladium (II) and gold (III) from aqueous solutions onto L-lysine modified crosslinked chitosan resin, J. Hazard. Mater., 146 (2007) 39–50.

[33] R. Qu, M. Wang, C. Sun, Y. Zhang, C. Ji, H. Chen, Y. Meng, P. Yin, Chemical modification of silica-gel with hydroxyl- or amino-terminated polyamine for adsorption of Au(III), Appl. Surf. Sci., 255 (2008) 3361–3370.

[34] M. Yu, D. Sun, W. Tian, G. Wang, W. Shen, N. Xu, Systematic studies on adsorption of trace elements Pt, Pd, Au, Se, Te, As, Hg, Sb on thiol cotton fiber, Anal. Chim. Acta., 456 (2002) 147–155.

[35] G. Gamez, J.L. Gardea-Torresdey, K.J. Tiemann, J. Parsons, K. Dokken, M.J. Yacaman, Recovery of gold (III) from multi-elemental solutions by alfalfa biomass, Adv. Environ. Res., 7 (2003) 563–571.

[36] D. Jermakowicz-Bartkowiak, B.N. Kolarz, A. Serwin, Sorption of precious metals from acid solutions by functionalised vinylbenzyl chloride-acrylonitryle-divinylbenzene copolymers bearing amino and guanidine ligands, React. Funct. Polym., 65 (2005) 135–142.

[37] M.M. Dubinin, E.D. Zaverina, L.V. Radushkevich, Sorption and structure of active carbons. I. Adsorption of organic vapors, Zh. Fiz. Khim., 21 (1947) 1351–1362.
[38] C.C. Wang, L.C. Juang, C.K. Lee, T.C. Hsua, J.F. Leeb, H.P. Chaob, Effects if exchanged surfactant cations on the pore structure and adsorption characteristics of montmorillonite, J. Colloid Interf. Sci., 280 (2004) 27–35.
[39] R. Donat, The removal of uranium (VI) from aqueous solutions onto natural sepiolite, J. Chem. Thermodyn., 41 (2009) 829–835.
[40] Y. Zhang, J. Chen, X. Yan, Q. Feng, Equilibrium and kinetics studies on adsorption of Cu(II) from aqueous solutions onto a graft copolymer of cross-linked starch/acrylonitrile (CLSAGCP), J. Chem. Thermodyn., 39 (2007) 862–865.
[41] S. Debnath, U.C. Ghosh, Kinetics, isotherm and thermodynamics for Cr(III) and Cr(VI) adsorption from aqueous solutions by crystalline hydrous titanium oxide, J. Chem. Thermodyn., 40 (2008) 67–77.
[42] Y.S. Ho, G. McKay, Sorption of dye from aqueous solution by peat, Chem. Eng. J., 70 (1998) 115–124.
[43] D. Bulgariu, L. Bulgariu, Equilibrium and kinetics studies of heavy metal ions biosorption on green algae waste biomass, Bioresour. Technol., 103 (2012) 489–493.
[44] E.I. Unuabonah, K.O. Adebowale, B.I. Olu-Owolabi, Kinetic and thermodynamic studies of the adsorption of lead (II) ions onto phosphate modified kaolinite clay, J. Hazard. Mater., 144 (2007) 386–395.
[45] A. Sari, M. Tuzen, Biosorption of total chromium from aqueous solution by red algae (Ceramium virgatum): Equilibrium, kinetic and thermodynamic studies, J. Hazard. Mater., 160 (2008) 349–355.
[46] C.H. Wu, Adsorption of reactive dye onto carbon nanotubes: Equilibrium, kinetics and thermodynamics, J. Hazard. Mater., 144 (2007) 93–100.

Supplemental materials

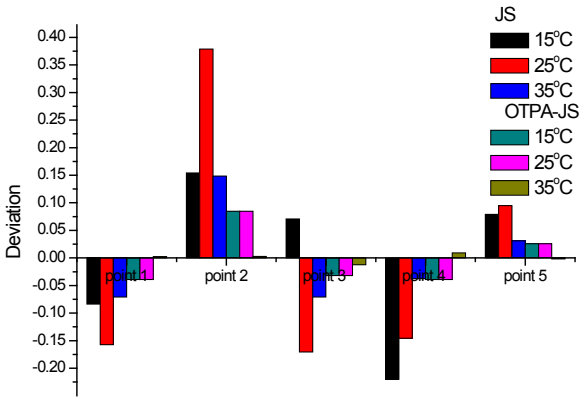

(a)

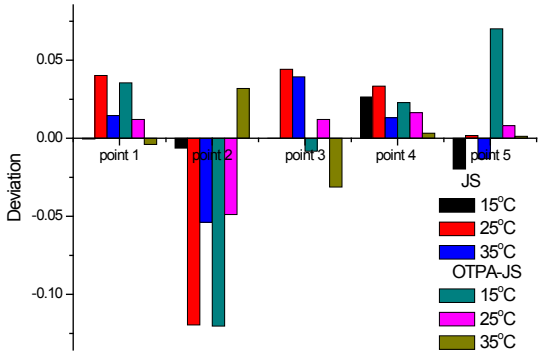

(b)

Fig. S1. Deviation of the fitted values and the experimental values for the Langmuir (a) and Freundlich (b) isotherms.

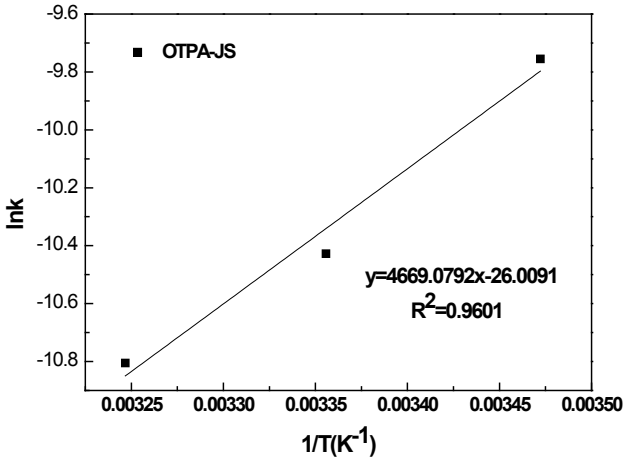

Fig. S2. Relationship between ln k and $1/T$ for OTPA-JS.

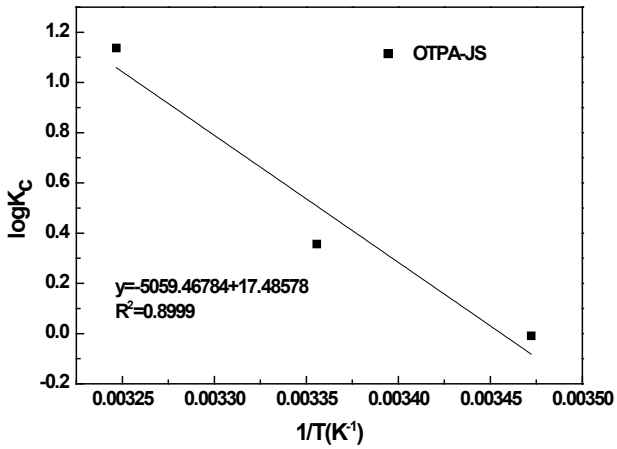

Fig. S3. log K_c *vs.* $1/T$ plot for Au(III) adsorption onto OTPA-JS.

Table S1
Selected geometrical parameters of the cellulose with organotriphosphonic acid group obtained at the B3LYP/6-31+G(d) level, and the atom labels are according to Fig. 1

Bond length (Å)	Bond angle (°)	Dihedral angle (°)
C1–C3 1.5322	A(1,3,7) 109.8	D(2,1,3,7) 57.8
C1–O5 1.4223	A(3,1,5) 112.0	D(4,1,3,7) –60.6
O5–H6 0.9725	A(1,3,17) 106.4	D(5,1,3,17) 57.4
C1–C4 1.5371	A(3,7,9) 110.1	D(2,1,4,21) 158.9
C3–C7 1.5479	A(3,7,19) 108.5	D(3,1,4,22) 157.0
C4–C10 1.5384	A(1,4,10) 109.0	D(16,3,7,8) 144.0
C7–O9 1.4375	A(1,4,22) 111.4	D(1,3,17,18) –163.5
O9–C10 1.4423	A(7,9,10) 111.9	D(1,4,10,9) 26.9
C10–C12 1.5201	A(4,10,9) 109.3	D(22,4,10,11) 147.3
C12–O15 1.4488	A(4,10,12) 115.5	D(8,7,19,20) 74.7
O15–P24 1.6281	A(10,12,15) 111.1	D(7,9,10,12) 160.3
P24–O26 1.6120	A(15,24,25) 113.0	D(4,10,12,15) 169.8
O26–H27 0.9814	A(15,24,26) 106.3	D(10,12,15,24) 64.2
P24–O25 1.5096	A(15,24,28) 104.0	D(12,15,24,25) –95.4
P24–C28 1.8346	A(25,24,28) 114.0	D(25,24,26,27) 54.7
C28–N31 1.4615	A(26,24,28) 103.3	D(24,28,29,30) 63.8
N31–C32 1.4594	A(24,28,29) 109.5	D(25,24,28,29) –175.2
N31–C35 1.4493	A(24,28,31) 110.2	D(24,28,31,32) 121.9
C32–P38 1.8437	A(28,31,32) 117.6	D(29,28,31,35) 31.5
P38–O41 1.4925	A(28,31,35) 116.5	D(28,31,32,38) –61.2
P38–O46 1.6252	A(31,32,33) 108.4	D(33,32,38,41) –164.2
P38–O48 1.6030	A(31,32,38) 112.0	D(36,35,39,44) 53.3
C35–P39 1.8475	A(32,38,41) 113.8	D(48,38,46,47) 108.9
P39–O40 1.4920	A(32,38,48) 106.1	D(32,38,48,49) 76.1
P39–O42 1.6343	A(31,35,39) 116.4	D(44,39,42,43) 125.9
P39–O44 1.6277	A(35,39,44) 101.5	D(35,39,44,45) 160.3

Table S2
Mulliken atomic charges of the cellulose with organotriphosphonic acid group at the B3LYP/6-31G+(d), and the atom labels are according to Fig. 1

Atoms	Charges	Atoms	Charges	Atoms	Charges
C1	−0.105	H18	0.498	C35	−0.808
H2	0.224	O19	−0.654	H36	0.249
C3	−0.272	H20	0.588	H37	0.270
C4	−0.117	H21	0.208	P38	1.709
O5	−0.652	O22	−0.697	P39	1.616
H6	0.498	H23	0.507	O40	−0.714
C7	0.390	P24	2.162	O41	−0.714
H8	0.198	O25	−0.966	O42	−0.805
O9	−0.571	O26	−0.864	H43	0.510
C10	0.377	H27	0.603	O44	−0.818
H11	0.251	C28	−0.938	H45	0.513
C12	−0.722	H29	0.288	O46	−0.841
H13	0.260	H30	0.305	H47	0.506
H14	0.226	N31	−0.188	O48	−0.790
O15	−0.602	C32	−0.781	H49	0.621
H16	0.231	H33	0.242		
O17	−0.677	H34	0.244		

Table S3
Data fitting of the adsorption equilibrium for gold ions by OTPA-JS at 25°C

Langmuir isotherm					
	q	K_L	SAE	ARE	SSE
SAE	400.025	10.542	124.541	0.0717	7571.139
ARE	400.025	10.542	124.541	0.0717	7571.139
SSE	389.299	11.058	141.639	0.0786	7112.106
LTFM	431.030	0.0604	233.245	0.225	34884.63
$R^2 = 0.9983$					
Freundlich isotherm					
	K_F	n	SAE	ARE	SSE
SAE	233.266	11.171	23.453	0.0142	404.657
ARE	233.266	11.171	23.453	0.0142	404.657
SSE	226.747	10.777	31.044	0.0212	307.053
LTFM	230.47	11.170	33.052	0.0197	337.938
$R^2 = 0.9916$					